

Quantum information processing using quasiclassical electromagnetic interactions between qubits and electrical resonators

Andrew J. Kerman

MIT Lincoln Laboratory, Lexington, MA 02420

(Dated: April 9, 2019)

Electrical resonators are widely used in quantum information processing with any qubits that are manipulated via electromagnetic interactions. In nearly all examples to date they are engineered to interact with qubits via real or virtual exchange of (typically microwave) photons, and the resonator must therefore have both a high quality factor and strong quantum fluctuations, corresponding to the strong-coupling limit of cavity QED. Although great strides in the control of quantum information have been made using this so-called “circuit QED” architecture, it also comes with some characteristic limitations. In this paper, we discuss a new paradigm for coupling qubits electromagnetically via resonators, in which the qubits do not exchange photons with the resonator, but instead where the qubits exert quasi-classical, effective “forces” on it. We show how this type of interaction is similar to that induced between the internal state of a trapped atomic ion and its center-of-mass motion by the photon recoil momentum, and that the resulting multiqubit entangling operations are insensitive *both to the state of the resonator and to its quality factor*. The method we describe is potentially applicable to a variety of qubit modalities, including superconducting and semiconducting solid-state qubits, trapped molecular ions, and possibly even electron spins in solids.

PACS numbers:

Microwave electrical resonators are already an important tool for manipulating quantum information using electromagnetic interactions [1]. As a means of quantum information storage or communication, they are used or proposed in a variety of schemes involving, for example, trapped molecular ions [2], neutral polar molecules [3], Rydberg atoms [4, 5], superconducting Josephson-junction qubits [6, 7], and electron spins in solids [8, 9]. In all of these cases, the resonator is used in a way familiar from optical cavity quantum electrodynamics [5, 10], in which the qubits exchange real or virtual photons with the cavity, and where the figure of merit is the speed with which this exchange occurs (or equivalently, the strength of the coherent qubit-cavity coupling). In fact, many of the seminal cavity QED results have been replicated in a circuit environment, a field now known as circuit QED [6, 7] (cQED).

Although this paradigm has been extremely fruitful for quantum information processing, it also presents some characteristic limitations in this context. For example, photon exchange can in most cases be controlled dynamically only by detuning the qubit from resonance with the cavity [11], which does not in general allow a very strong suppression when the coupling is intended to be off. In addition, whenever exchange of photons is possible between the qubit and other circuit elements, including but not limited to resonators, additional pathways open for the qubit’s excited state to decay, by emitting photons into environmental degrees of freedom associated with those elements [12]. Finally, since cQED exploits a strong, manifestly quantum interaction between qubit and resonator, and effectively uses the resonator to store or transport quantum information, its protocols are sensitive both to spurious population of excited resonator quantum levels, and to spontaneous decay of those lev-

els. High fidelity in cQED quantum operations therefore requires both a correspondingly high cavity quality factor Q , as well as strong suppression of the spurious population of excited levels which is typically encountered in experiments [13].

In this paper, we describe a different paradigm for using electrical resonators to couple (possibly distant) qubits via electromagnetic interactions, which *does not involve any photon exchange* between resonator and qubits, and therefore largely avoids these limitations. Our proposal is built on an analogy with demonstrated methods [14, 15] developed by Mølmer and Sørensen [16] and Milburn [17] for entangling trapped atomic ions via their collective center-of-mass vibrational modes [18, 19]. In contrast to cQED as described above, here we manipulate only quasi-classical resonator states whose vacuum fluctuations can be small, using purely classical, qubit-state-dependent forces [20]. As a result, the resonator can be treated classically, its initial state is almost irrelevant to the protocol, and high quality factors are no longer required.

In section I below, we describe the general qubit-resonator system under consideration. Section II contains a detailed description of how entangling operations can be achieved between qubits coupled to a common resonator, without any exchange of photons as in cQED. In section III we consider in detail the leading sources of error in two-qubit entangling operations, and evaluate these errors for a variety of different physical qubit modalities, which are tabulated in table I. We conclude in section IV with a comparison to the methods used with trapped ions, as well as cQED. In the appendix we describe the assumptions and parameter values used to evaluate the gate errors shown in the table.

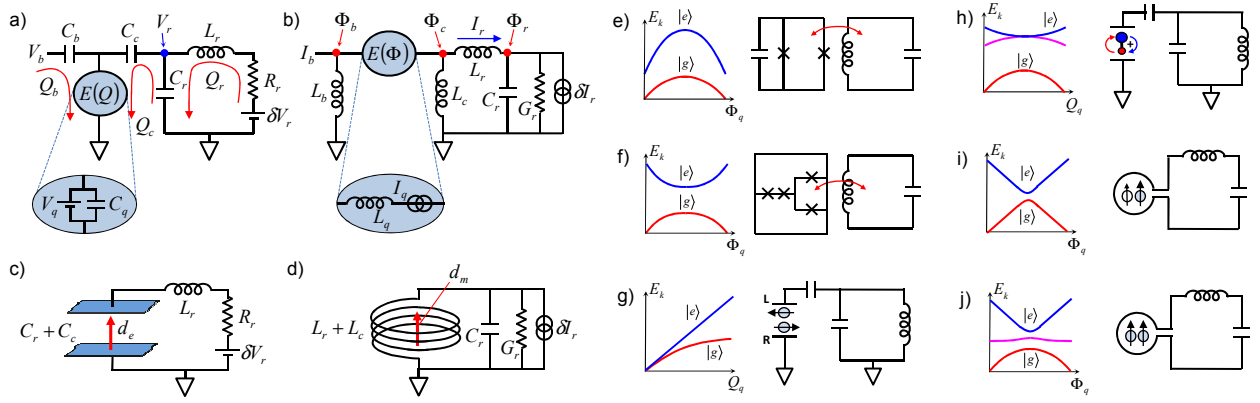


FIG. 1: Electromagnetic qubit/resonator coupling without exchange of photons. (a) shows the electric circuit analyzed in detail; (b) is its exact dual [22, 23], governed by equations of identical form, via the transformation: $Q \leftrightarrow \Phi, C \leftrightarrow L, V \leftrightarrow I, Y \leftrightarrow Z$ [24], in which loop charges [red arrows in (a)] become node fluxes [red dots in (b)] [25]. The qubit states $|e\rangle$ and $|g\rangle$ have stationary energies $E_g(p)$ and $E_e(p)$, classical functions of $p \in Q_q, \Phi_q$, and are described in (a) by a parallel state-dependent voltage source V_q and capacitance C_q (defined in the text), and in (b) by a series state-dependent current source I_q and inductance L_q . Resonator damping, and the associated fluctuations, are modeled in (a) via R_r and the Langevin noise source δV_r , and in (b) by G_r and δI_r . (c) and (d) show classical systems analogous to the circuits of (a) and (b), in which an electric or magnetic dipole is placed inside the resonator, producing an orientation-dependent displacement. (e)-(j) show examples of physical qubits coupled to resonators in the manner of our proposal (the qubit bias is not shown) as well as the energies $E_g(p)$ and $E_e(p)$ schematically [see the appendix for details]. (e) tunable transmon [6, 7] (f) tunable flux qubit [26, 27] (g) singlet-triplet double quantum dot [28–30]; (h) polar molecular ion [2], where the third curve (shown in magenta) corresponds to the two degenerate $J = 1, m_J = \pm 1$ levels; (i) ^{31}P coupled electron and nuclear spins in ^{28}Si [31], where we show only one nuclear spin orientation. The splitting at zero field is due to hyperfine coupling; (j) Nitrogen-vacancy center in diamond [32], with a fixed transverse magnetic field, as a function of an additional longitudinal field. The third (magenta) curve shows the two degenerate levels which become $m_S = 0$ in the limit of large longitudinal field.

I. GENERAL QUBIT-RESONATOR SYSTEM

We first consider a microwave resonator coupled to a single qubit, as illustrated in figs. 1(a) and (b) for capacitive and inductive qubit/resonator coupling. These two circuits are chosen to be exactly *dual* [22, 23], so that the solution for one case can be mapped directly to the other using the transformation: $Q \leftrightarrow \Phi, C \leftrightarrow L, V \leftrightarrow I, Y \leftrightarrow Z$. The qubit-resonator interaction of interest to us is of a quite general form, in which the qubit's stationary energy levels $|g\rangle$ and $|e\rangle$ have energies $E_g(p)$ and $E_e(p)$ with a specified, *classical* dependence on the parameter p , which is typically the flux through a qubit loop or the charge on a gate electrode, induced by the resonator. We are interested here in cases where any interaction by which the qubit can exchange photons with the resonator can be neglected, several examples of which are shown in figs. 1(e)-(j). We consider the capacitively-coupled circuit of fig. 1(a), and write the classical potential energy in terms of the loop charges Q_b, Q_c, Q_r [25] (for the moment taking $R_r, \delta V_r \rightarrow 0$):

$$U(Q_r, Q_c, Q_b) = E_q(0) + \frac{(Q_r - Q_c)^2}{2C_r} + \frac{Q_c^2}{2C_c} + \frac{Q_b^2}{2C_b} + \underbrace{\int_0^{Q_q} V_q(Q'_q) dQ'_q - \int_0^{Q_b} V_b(Q'_b) dQ'_b}_{E_q(Q_q) - E_q(0)} \quad (1)$$

where $E_q(Q_q)$ is the qubit energy, $Q_q \equiv Q_b + Q_c$, and $V_q(Q_q) \equiv dE_q/dQ_q$ is the voltage across it; $V_b(Q_b)$ is the bias voltage which corresponds to Q_b . The terms in the second line are the potential energies of the qubit and the source, respectively, and can be viewed as work done by (or on) the source as V_b is turned up from zero.

We now seek to write eq. 1 in terms of deviations of the charges Q_n ($n \in b, c, r$) from the minimum energy solution Q_{n0} , given by: $Q_{b0} = C_b(V_b - V_q)$, $Q_{c0} = -C_c V_q$, $Q_{r0} = Q_{c0}$ (which must be obtained self-consistently since V_q depends implicitly on Q_q). Note that $U(Q_{r0}, Q_{c0}, Q_{b0})$ is a constant, independent of V_b , as required by total energy conservation. Writing: $Q_n \equiv Q_{n0} + \delta Q_n$, we then expand the qubit energy:

$$E_q(Q_{q0} + \delta Q_q) \approx E_q(Q_{q0}) + V_q \delta Q_q + \frac{\delta Q_q^2}{2C_q} + \dots \quad (2)$$

where $C_q \equiv (d^2 E_q / dQ_q^2)^{-1}$ is the effective dynamic capacitance of the qubit at Q_{q0} . We emphasize that V_q and C_q depend on the internal state of the qubit, in addition to its bias. Of the three δQ_n , only δQ_r is an independent dynamical variable, since it couples to an inductance (the effective “mass” for a fictitious particle whose “position” is δQ_r [23, 25?]), while δQ_b and δQ_c are deterministically related to δQ_r . To determine these relations, we hold V_b and δQ_r fixed and minimize U with respect to δQ_c and δQ_b , to obtain: $\delta Q_b = 0$ and

$\delta Q_r/C_r = \delta Q_c(C_r^{-1} + C_c^{-1} + C_q^{-1})$. Combining this with eqs. 1-2, we find:

$$U = \frac{(Q_r + C_c V_q)^2}{2C'_r} \quad (3)$$

with the qubit-state-dependent quantities (via C_q [33]):

$$C'_r \equiv C_r + \frac{C_c C_q}{C_c + C_q}$$

$$\omega_r \equiv \frac{1}{\sqrt{L_r C'_r}}, \quad Y_r \equiv \sqrt{\frac{C'_r}{L_r}} = \frac{1}{Z_r} \quad (4)$$

Thus, the qubit effectively exerts a state-dependent “force” on the oscillator, displacing its equilibrium “position” by an amount $C_c V_q$, without changing the total energy at that position. It may at first seem strange that a quasistatic displacement of Q_r is possible at all, since L_r would appear to act as a short across C_r at low frequencies (for $R_r, \delta V_r = 0$). However, Q_r (which we choose to be the canonical position variable of the resonator), is *not* simply the charge on the capacitor C_r . Rather, Q_r is more precisely a *quasicharge* [23], defined in this case by: $dQ_r/dt = I_r + C_r dV_r/dt$, whose conjugate momentum is the inductor fluxoid Φ_r defined here by: $d\Phi_r/dt = V_r - L_r dI_r/dt$. A nonzero quasistatic displacement of Q_r is therefore possible due to a nonzero time-integral of the *displacement current* $C_r dV_r/dt$.

To see intuitively how this arises, we can map our problem onto a more familiar electrostatic system, as shown in fig. 1(c): that of an electric displacement $C_c V_q$ contained inside the capacitor C_r . We can imagine this as an electric dipole which was moved into the capacitor (with its orientation held fixed), such that the resulting transient voltage appearing across C_r gives $\int C_r (dV_r/dt) dt = C_c V_q$ (analogous arguments apply to the magnetic case in fig. 1(b) for a qubit with $dE/d\Phi \equiv I_q \neq 0$, which acts like a magnetization inside the resonator inductor L_r , as in fig. 1(d)). This mechanical analogy casts the work done by the source (the second line of eq. 1) into the form of a potential energy associated with “assembling” the system, as is often encountered in electro- or magnetostatic problems: as a permanent electric dipole is moved into the resonator capacitor, there will be a mechanical force on that dipole due to the gradient of potential energy in real space, such that work must be done while moving the dipole into position. In our system, this “motion” consists of turning up the bias voltage V_b .

The form of eq. 3 can now be used as the basis for an analogy between our coupled qubit/resonator system and a harmonically trapped atom whose internal states are coupled to its center-of-mass motion by the photon recoil momentum. In the latter case, this coupling occurs typically in one of two ways: (i) via Rayleigh scattering of laser photons tuned near resonance with an electronic transition from an incident laser wavevector \mathbf{k}_L to

\mathbf{k}' , which imparts a recoil momentum $\hbar(\mathbf{k}_L - \mathbf{k}')$ (radiation pressure) and can be used to implement dissipative laser cooling of the atomic motion [34]; or (ii) via coherent (stimulated) scattering far from resonance (the so-called “dipole force” [35]), which can be used to realize essentially non-dissipative forces with internal-state-dependence. Here we focus on the latter case [36].

II. CONTROLLED-PHASE GATE WITH QUASICLASSICAL FORCES

Following refs. 14–17, we describe the oscillator in terms of the dimensionless classical field amplitude: $\alpha = \langle \hat{u} + i\hat{v} \rangle$, where:

$$\hat{u} \equiv \frac{\hat{Q}_r}{\sqrt{\hbar Y_r}} = \frac{\hat{a} + \hat{a}^\dagger}{\sqrt{2}}$$

$$\hat{v} \equiv \frac{\hat{\Phi}_r}{\sqrt{\hbar Z_r}} = \frac{\hat{a} - \hat{a}^\dagger}{i\sqrt{2}} \quad (5)$$

and Φ_r is the resonator flux (associated with L_r), the canonical momentum of the oscillator such that $[\hat{u}, \hat{v}] = i$. The quantity α is a c-number for coherent states, while in the presence of statistical (e.g. thermal) fluctuations of the field it can be written as a diagonal density matrix (in the Glauber-Sudarshan P -representation [37]). When we couple N qubits to our resonator, in general all resonator quantities become operators in the 2^N -dimensional qubit Hilbert space: $\alpha \rightarrow \hat{\alpha}$, $\omega_r \rightarrow \hat{\omega}_r$, $Z_r \rightarrow \hat{Z}_r$, $Y_r \rightarrow \hat{Y}_r$. In the cases of interest to us here, these operators are all *diagonal*, and commute with the individual qubit Hamiltonians [38].

We wish to focus on the qubit-state-dependent dynamics of the operator $\hat{\alpha}$, while the state dependence of the other resonator quantities are higher-order effects which we will consider as perturbations only, in section III. To that end, we define:

$$\hat{\omega}_r \equiv \tilde{\omega}_r (1 + \delta \hat{\omega}_r) \quad (6)$$

where $\tilde{\omega}_r \equiv \text{Tr}[\rho_m \hat{\omega}_r]$, and $\rho_m \equiv \hat{I}_{2^N}/2^N$ is the completely mixed state of the N qubits (\hat{I}_d is the d -dimensional identity matrix). This definition separates the *average* effect on the resonator due to coupling to the qubits (which is simply a renormalization of its frequency and impedance) from qubit-state-dependent effects. We can now write the equation of motion for the oscillator with quality factor Q as [39]:

$$\frac{d\hat{\alpha}}{d\tau} = -i(1 + \delta \hat{\omega}_r)[\hat{\alpha} - \hat{\eta}] - \frac{\hat{\alpha} - \hat{\alpha}^*}{2Q} \quad (7)$$

where $\tau \equiv \tilde{\omega}_r t$, we have made the following replacements in eqs. 5 above: $Z_r = 1/Y_r \rightarrow \hat{Z}_r = 1/\hat{Y}_r = \hat{\omega}_r L_r$, and we

can write the dimensionless, qubit-state-dependent frequency shift and force as:

$$\begin{aligned}\delta\omega_r &\equiv \sum_{i=1}^N \delta\omega_r^- \hat{\sigma}_i^z \\ \hat{\eta} &\equiv \sum_{i=1}^N \left[(\eta^- + \delta\eta^-) \hat{\sigma}_i^z + (\eta^+ + \delta\eta^+) \hat{I}_i \right] \quad (8)\end{aligned}$$

where $i \in 1 \dots N$ indexes the qubits, $\hat{\sigma}_i^z$ and \hat{I}_i are the Pauli- z and identity operator for qubit i , and:

$$\begin{aligned}\delta\omega_r^- &\approx \frac{\beta_r \beta_q^-}{4} \\ \beta_r &\equiv \frac{C_c}{C_c + C_r}, \quad \hat{\beta}_q \equiv \frac{C_c}{C_c + \hat{C}_q} \\ \eta^\pm &\approx \frac{C_c V_q^\pm}{2\sqrt{\hbar Y_r}} \quad (9)\end{aligned}$$

using the notation: $X^\pm \equiv [\langle e|\hat{X}|e\rangle \pm \langle g|\hat{X}|g\rangle]/2$ with \hat{X} a single-qubit operator. For the sake of clarity we have assumed all N qubits and coupling elements are identical (though the method we propose does not require this), and we have retained only the leading order term in $\delta\omega_r^- \ll 1$ (we will see in table I below that this is a very good approximation). Note that there is no nonzero $\delta\omega_r^+$ because of our definition of $\tilde{\omega}_r$ [c.f., eq. 6]. The quantities $\delta\eta^\pm$ are Langevin noise terms, with $\delta\eta^-$ due to qubit bias noise, and $\delta\eta^+$ associated with the finite resonator Q . In our model [fig. 1(a)] the latter comes from the Johnson-Nyquist noise δV_r of the resistance R_r ($Q = Z_r/R_r$). The resulting dimensionless noise power spectral density of the fluctuating force $\delta\eta^+$ can be written:

$$\begin{aligned}S_{\delta\eta^+}(\Omega) &= \frac{C_r^2 \tilde{\omega}_r}{\hbar Y_r} \langle \delta V_r(t) \delta V_r(t') \rangle_\omega \\ &= \frac{2\Omega}{Q} \coth\left(\frac{\Omega \tau_c}{2}\right) \quad (10)\end{aligned}$$

where the brackets denote an environment average, the subscript ω indicates a Fourier transform, $\Omega \equiv \omega/\tilde{\omega}_r$ is dimensionless frequency, and $\tau_c \equiv \hbar \tilde{\omega}_r / k_B T_r$ with T_r the effective resonator mode temperature.

To implement a multiqubit gate, following the trapped ion case [14, 16], we use time- and qubit-state-dependent forces on the oscillator, which result in qubit-state-dependent paths of the oscillator in u, v phase space. Each amplitude in the N -qubit wavefunction then acquires a geometric phase associated with the corresponding oscillator path, given by the phase space area it encloses: $\hat{\phi}_g = \text{Im}[\oint \hat{\alpha}^* d\hat{\alpha}]$. To produce the forces, we drive all of the qubits simultaneously with an oscillatory bias [40]: $Q_{b0} = Q_{DC} + \delta Q_{AC} \sin(\omega_d t)$, such that the corresponding state-dependent force on the oscillator is:

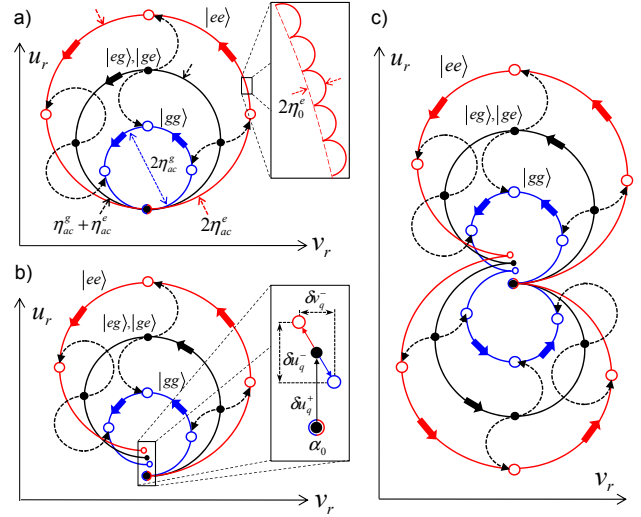


FIG. 2: Oscillator phase space trajectories due to classical “forces” exerted by two qubits. Trajectories are shown in a frame rotating at $\tilde{\omega}_r$, and the area enclosed within each path, indicated by solid lines ($|gg\rangle$ - blue, $|eg\rangle, |ge\rangle$ - black, $|ee\rangle$ - red) is the geometric phase acquired by that amplitude of the qubits’ internal-state wavefunction. Dashed arrows show the displacements of $|ee\rangle$ and $|gg\rangle$ relative to $|ge\rangle, |eg\rangle$, to make a connection between the general case considered here where $\langle eg|\hat{\eta}|eg\rangle, \langle ge|\hat{\eta}|ge\rangle \neq 0$, and the usual situation in the trapped-ion case $\langle eg|\hat{\eta}|eg\rangle, \langle ge|\hat{\eta}|ge\rangle = 0$ [14–16]. (a) In the ideal case ($Q \rightarrow \infty, \delta\omega_r = 0$), the paths are closed. The inset shows the high-frequency component of the response due to the counter-rotating term in eq. 11. (b) for finite $Q, \delta\omega_r$, the trajectories are no longer closed, such that at the end of the gate a nonzero total oscillator displacement $\delta\alpha_q^-$ is entangled with the qubits’ internal state. The inset shows the components $\delta u_q^\pm, \delta v_q^\pm$ of this residual displacement ($\delta v_q^+ = 0$ because $\delta\omega_r^+ = 0$); finite decay results in a shrinking radius of the path with time, producing finite δu_q^- at the end of the gate, and finite $\delta\omega_r$ makes the drive detuning δ_d weakly qubit-state-dependent, producing a nonzero δv_q^- . (c) modified gate sequence where either the force is reversed, or the qubits are inverted, in the middle of the gate, such that at the end of the gate the spurious entanglement between qubits and oscillator is removed.

$\hat{\eta} = \hat{\eta}_0 \sin(\omega_d t)$ (for a drive centered on a bias point where $\hat{V}_q^- = 0$, a so-called “degeneracy point” [41]). Neglecting for the moment the finite Q , fluctuations $\delta\eta^\pm$, and frequency shift $\delta\omega_r^-$, and taking the drive to be turned on at $\tau = 0$ with the oscillator in the state α_0 and not entangled with the qubit, we find (in a frame rotating at $\Omega_d \equiv \omega_d/\tilde{\omega}_r$):

$$\begin{aligned}\hat{\alpha} &= \hat{I}_N \alpha_0 e^{i\delta_d \tau} + i\hat{\eta}_{ac} \left[(\Omega_d e^{i\delta_d \tau} - 1) - \frac{\delta_d}{2} (e^{i2\Omega_d \tau} + 1) \right] \\ \hat{\eta}_{ac} &\equiv \frac{\hat{\eta}_0}{\delta_d (2 + \delta_d)} \quad (11)\end{aligned}$$

where the detuning δ_d of the drive is defined according to: $\omega_d \equiv \tilde{\omega}_r (1 + \delta_d)$. In eq. 11, the first term is free evo-

lution, and the second and third terms can be viewed as the co- and counter-rotating components of the oscillator response, respectively, due to the effective force $\hat{\eta}_{ac}$.

The resulting oscillator dynamics in phase space, for a two-qubit system, are shown in fig. 2(a). The entanglement of the oscillator with the qubits vanishes when the trajectories return to their initial point, at times τ satisfying the conditions:

$$\frac{\delta_d \tau}{2\pi} = m, \quad \frac{\tau}{2\pi} = \frac{k}{2} \quad (12)$$

where m, k are integers ($k > 2m$). During this time the system has accrued a state-dependent geometric phase, given by (neglecting overall phases):

$$\hat{\phi}_g = \frac{2\pi m}{\delta_d^2(2 + \delta_d)} [(\eta_0^-)^2 \hat{\sigma}_1^z \hat{\sigma}_2^z + 2\eta_0^- \eta_0^+ (\hat{\sigma}_1^z + \hat{\sigma}_2^z)] \quad (13)$$

A controlled- π gate, sufficient in combination with single-qubit gates for universal quantum operations, is implemented (in addition to the single-qubit phase shifts given by the second term in eq. 13) if we choose:

$$\eta_0^- = \delta_d \sqrt{\frac{2 + \delta_d}{4m}} \quad (14)$$

where the total gate time is, to leading order in δ_d^{-1} :

$$\frac{\tau_\pi}{2\pi} \approx \sqrt{\frac{m}{2}} \frac{1}{\eta_0^-} \quad (15)$$

Obviously, choosing $m = 1$ gives the fastest possible gate for a given η_0^- ; however, as we will see, this choice in most cases does not give the lowest gate error.

Before discussing realistic errors in these operations, we highlight some distinctions between the type of coupling we are discussing, and that used in cQED [6, 7]. First, the coupling strength [c.f., eq. 9] here depends only on the resonator admittance, and not on its resonant frequency, as compared to cQED where the detuning of the qubit from the resonator controls the strength of the coupling. This difference is a direct consequence of the fact that in our scheme no photons are exchanged between resonator and qubit. In addition, here the coupling strength is *inversely* proportional to the vacuum fluctuation amplitude of the oscillator $\sqrt{\hbar Y_r}$, such that the larger the classical displacement of the oscillator compared to its quantum fluctuations, the stronger the coupling; By contrast, in circuit QED, the opposite is true: for example, in the case of a transmon qubit coupled capacitively to a resonator, the transverse coupling strength can be written: $g \propto \beta_r \sqrt{\hbar Y_r}$ - strong interaction corresponds to the case where quantum fluctuations dominate and classical displacements are absent (this is precisely the strong coupling limit in which circuit QED becomes

possible). An important consequence of this is that in circuit QED spurious population of resonator excited states (equivalently, nonzero resonator temperature) linearly affects gate fidelity, whereas in our scheme it has only a higher-order effect for statistical fluctuations, and no effect for coherent resonator excitation. This difference may be important since not only is it difficult to completely remove spurious excited-state populations [13], but it is also much harder to achieve very high resonator Q at the single-photon level than it is when the resonator is strongly driven [42].

III. TWO-QUBIT GATE FIDELITY

We now seek to evaluate the constraints on the two-qubit gate fidelity, and examples of our results are tabulated in table I for several qubit modalities. We begin with the effect illustrated in fig. 2(b), spurious entanglement between qubits and resonator at the end of the gate in the form of a residual qubit-state-dependent oscillator displacement $\delta\alpha_q^-$. The two mechanisms which produce this type of entanglement are finite resonator Q , and the state-dependent frequency shift $\delta\hat{\omega}_r$. As shown in fig. 2(b), resonator decay causes the radius of the phase-space trajectory to shrink with time, while $\delta\hat{\omega}_r$ effectively produces a detuning δ_d (and corresponding evolution rate around the paths in phase space) which is qubit-state-dependent. We can bound the resulting error $\epsilon_{\delta\alpha}$ using the fidelity [43] between the desired qubit density matrix after the gate ρ_f^{qb} and the actual total density matrix after the gate ρ_f^{tot} , traced over resonator states [44]:

$$\epsilon_{\delta\alpha} \approx 1 - \left(\text{Tr} \left[\sqrt{(\rho_f^{qb})^{1/2} \text{Tr}_r[\rho_f^{tot}] (\rho_f^{qb})^{1/2}} \right] \right)^2 \quad (16)$$

$$\begin{aligned} \rho_f^{tot} &\equiv D_Q^\dagger \left[\rho_f^{qb} \otimes D^\dagger(\alpha_0 + \delta\alpha_q^+) \rho_{th}^r D(\alpha_0 + \delta\alpha_q^+) \right] D_Q \\ D_Q &\equiv D \left[+\frac{\delta\alpha_q^-}{2} \right] |gg\rangle\langle gg| + D \left[-\frac{\delta\alpha_q^-}{2} \right] |ee\rangle\langle ee| \end{aligned}$$

where ρ_{th}^r is a thermal resonator state with temperature T_r , $D(\delta\alpha)$ is the displacement operator in u, v phase space for (complex) displacement $\delta\alpha$, and D_Q performs the state dependent displacement shown in fig. 2(b). Note that in the presence of damping, α_0 is nonzero only if the resonator is driven. As an approximate worst case estimate, we take: $\rho_f^{qb} = (|gg\rangle + |ee\rangle)(\langle gg| + \langle ee|)/2$, and find (using the results of ref. 45):

$$\epsilon_{\delta\alpha} \approx \frac{|\delta\alpha_q^-|^2}{4} (1 + 2\bar{n}) \quad (17)$$

to leading order in $\delta\alpha_q^-$ and $\bar{n} \approx \exp(-\hbar\omega_r/k_B T_r)$, the mean thermal photon number in the resonator, and independent of $\alpha_0 + \delta\alpha_q^+$.

Now, for the gate shown in fig. 2(b), the finite Q and $\delta\hat{\omega}_r$ result in displacements: $\delta u_q^- \sim \mathcal{O}(1/Q)$ and

$\delta v_q^- \sim \mathcal{O}(\delta\omega_r^-)$, respectively. However, since both of these displacements result from classical and deterministic dynamics, we can strongly suppress them using the scheme shown in fig. 2(c). We divide the gate excitation into two periods of equal duration (*each* of which satisfies eqs. 12), and we switch the sign of the effective force η_{ac} between these two periods (alternatively, one could insert π -pulses to invert the qubits instead). This simple procedure works like a spin-echo, in the sense that the classical modifications to the trajectories cancel out at the end of the operation, such that the leading terms $\sim \mathcal{O}(1/Q), \mathcal{O}(\delta\omega_r^-)$ cancel. To evaluate the result quantitatively, we first renormalize the oscillator resonance frequency to account for the usual Q -induced shift:

$$\tilde{\omega}_r \rightarrow \tilde{\omega}_r \sqrt{1 - \frac{1}{4Q^2}} \quad (18)$$

and correspondingly renormalize the dimensionless time τ [eq. 7], drive frequency ω_d , detuning δ_d , and the conditions for m and k [eq. 12]. The final result, to leading order in the small quantities $\delta_d, \eta_0^-, Q^{-1}, \delta\omega_r^-$, is:

$$|\delta\alpha_q^-|^2 \approx mx^4 \left[1 + 2m \left(\frac{2\pi\delta\omega_r^-}{x} \right)^2 \right] \quad (19)$$

where $x \equiv \pi/(Q\eta_0^-)$ and m now includes both halves of the gate. As we show in table I, this echo procedure reduces $\epsilon_{\delta\alpha}$ to very low levels for all of the cases considered.

In addition to the displacement δv_q , the state-dependent frequency shift $\delta\omega_r^-$ also produces direct decoherence due to thermal photon-number fluctuations. Since this shift can be viewed as an n -dependent qubit frequency: $\omega_{qb} + 2n\delta\omega_r^-$, each qubit experiences dephasing at the rate [6]:

$$\Gamma_\phi \approx 16\tilde{\omega}_r\bar{n}Q(\delta\omega_r^-)^2 \quad (20)$$

for a thermal photon number distribution at temperature T_r with mean photon number \bar{n} [46]. Notice that the dephasing rate *increases* with increasing resonator Q , as the discrete frequencies associated with different photon number states become more resolved [6, 13].

We now consider the classical fluctuations $\delta\eta^\pm$ of the force during the gate, which arise both from the damping and possibly from qubit bias noise. For small fluctuations about the desired values, the system will accrue an additional geometric phase:

$$\delta\phi_g \approx 2 \int \left\{ \delta\eta^- [\eta^+ (\hat{\sigma}_1^z + \hat{\sigma}_2^z) + \eta^- \hat{\sigma}_1^z \hat{\sigma}_2^z] + \delta\eta^+ [\eta^- (\hat{\sigma}_1^z + \hat{\sigma}_2^z)] \right\} d\tau \quad (21)$$

where the three terms are: single- and two-qubit phase errors due to fluctuations of the state-dependent force

(qubit bias noise), and single-qubit errors due to oscillator fluctuations (as well as qubit bias noise if $V_q^+ \neq 0$). Since η^\pm oscillate at ω_d , and only noise which occurs at or near this high frequency or its harmonics will produce errors, in nearly all cases low-frequency qubit bias noise (e.g. 1/f charge or flux noise) can be ignored in this context. The oscillator noise, however, can be quite important as the Q is reduced, producing an average error (per qubit): $1 - F \approx \langle \delta\phi_g^2 \rangle = \int S_{\delta\eta^+}(\Omega) |\eta^-(\Omega)|^2 d\Omega$ where $\eta^-(\Omega)$ is the Fourier transform of $\eta^-(\tau)$, a peaked function centered on Ω_d , of width $\sim (2\tau_f)^{-1}$ and amplitude $\sim \eta_0^- \tau_f$. We obtain:

$$\epsilon_{\delta\eta^+} \sim \frac{\pi}{\sqrt{2mQ\eta_0^-}} \coth \frac{\tau_c}{2} \quad (22)$$

These errors will tend to restrict how small a Q can be used for these gates [47].

For qubits without a degeneracy point, such as singlet-triplet quantum dots [28–30], there will be an additional error contribution from the Q or Φ sensitivity associated with a nonzero η , in the presence of noise in these parameters. Of course, this type of error will always be present for such qubits independently of our scheme, so that decoupling schemes will be required [48] in any case. Here, the simplest such scheme would be to replace the reversal of η in the middle of the controlled- π gate with a π -pulse, exchanging the roles of $|g\rangle$ and $|e\rangle$ for each qubit (similar to ref. 30). In the limit where the π -pulse is much shorter than the gate time, this will produce the same effect as shown in fig. 2(c), as well as the usual spin-echo to remove the effect of quasistatic noise [30, 41].

Looking back at eqs. 17–22, we conclude that: (i) larger forces η_0^- are better; and (ii) higher-frequency resonators are better, for faster gates, lower \bar{n} , and so that $\hbar\omega_r \gg k_B T$ ($\tau_c \gg 1$). Some specific examples are shown in table I, where we attempt to illustrate the utility of our scheme over a range of qubit types, resonator Q 's, resonance frequencies, and photon populations \bar{n} . Note that in some cases two-qubit error rates as low as 10^{-3} are still achievable with Q as low as 25,000 or \bar{n} as high as 0.4, illustrating the robustness of our technique against resonator decay and fluctuations. With state-of-the-art resonator Q 's of 10^6 and low \bar{n} , even lower error rates $\sim 10^{-4}$ become accessible (provided that single-qubit errors unrelated to the operations considered here do not limit the gate).

In this context it is important to note that while very high resonator Q 's of 10^6 or greater are at present difficult to achieve in planar geometries at the single-photon level required for cQED implementations, this difficulty is substantially reduced at higher resonator powers ($\sim 10^3$ – 10^4 photons) where parasitic, lossy defects become saturated [42]. Given that our proposed method is not affected by a coherent initial resonator state, we can consider the prospect of intentionally driving the resonator to increase

qubit type	Q	$\omega_r/2\pi$ [GHz]	L_r [pH]	C_r [pF]	η_0^- [$\times 10^3$]	δ_d [$\times 10^3$]	m	Γ_ϕ^{-1} [ms]	t_π [ns]	$\epsilon_{\delta\alpha}$ [$\times 10^3$]	$\epsilon_{\delta\eta^+}$ [$\times 10^3$]	ϵ_{2qb} [$\times 10^3$]	Δ_{hm} [GHz]	N_γ
Flux	25000	10	250	0.84	4.5	64	100	8.4	160	0.015	2.0	2.0	2.3	2600
[26]	10^6	10	500	0.46	3.4	12	6	0.76	51	10^{-9}	0.27	0.34	3.5	5200
	10^6	1	30nH	0.84	1.4	2.9	2	0.23	700	2×10^{-8}	2.0	5.0	0.03	3.1×10^6
Transmon	50000	10	250	0.84	1.4	14	50	126	360	0.053	4.5	4.6	0.4	10^4
[12]	10^6	10	250	0.84	1.4	6.2	10	6.3	160	7×10^{-8}	0.51	0.53	0.9	10^4
	10^6	3	1500	1.8	1.1	2.2	2	0.10	300	3×10^{-8}	1.5	4.5	0.07	2.0×10^5
S-T QDs	25000	15	100nH ^a	1.1fF	3.0	33	60	3.0	120	0.20	3.8	4.0	1.4	2.5
[28–30]	10^6	15	30nH ^a	3.7fF	1.7	6.6	8	0.83	80	5×10^{-7}	0.47	0.57	1.4	8.5
CaCl ⁺ [2]	10^6	1	1000nH ^a	25fF	0.14	1.1	30	25s	27 μ s	0.0032	5.1	5.1	0.01	2.4×10^9
³¹ P- ²⁸ Si [31]	10^7	1	100 ^b	250	0.014	0.14	50	2×10^7 s	350 μ s	0.005	4.0	4.0	0.5 MHz	2.4×10^9
NV [32]	10^7	1	100 ^b	250	0.028	0.13	10	2s	78 μ s	6×10^{-5}	4.4	4.5	0.8 MHz	2.4×10^9

^a Impedances this high require the use of high-kinetic-inductance materials [54, 55]. Limits on achievable resonator Q and impedance for these materials are as yet unknown.

^b Impedances this low may not be achievable in a transmission-line resonator.

TABLE I: Selected examples of two-qubit controlled- π gate parameters (Details for each system are contained in the appendix). For transmission-line resonators, L_r and C_r are effective values for a given longitudinal mode. The results for gate errors shown are the thermal photon-number dephasing rate Γ_ϕ [eq. 20] (which is present due to the coupling even when no two-qubit gates are being driven), the gate time t_π [eq. 15], the state-dependent displacement error $\epsilon_{\delta\alpha}$ [eqs. 17,19] and the resonator fluctuation error $\epsilon_{\delta\eta^+}$ [eq. 22]. The total two-qubit error is defined as: $\epsilon_{2qb} \equiv 2\Gamma_\phi t_\pi + \epsilon_{\delta\alpha} + \epsilon_{\delta\eta^+}$. This does not include single-qubit errors unrelated to the coupling (for example, T_1 relaxation for the superconducting qubits or charge-noise dephasing for the quantum dots). The quantity Δ_{hm} is the minimum detuning to the next higher oscillator mode, if we assume it has the same Lamb-Dicke parameter as the fundamental, such that we the associated error $\epsilon_{hm} \leq 0.1 \times \epsilon_{2qb}$ [eq. 23]. In all cases we take a resonator temperature of $T_r = 40$ mK, corresponding to $\bar{n} = 0.4, 0.03, 4 \times 10^{-6}, 10^{-8}$ for $\omega_r/2\pi = 1, 3, 10, 15$ GHz. Note that both donor spins in Si and NV centers in diamond do not themselves require low temperatures, but here they are required to suppress errors due to classical, thermal resonator fluctuations [c.f., eqs. 22, 20]).

the effective Q for gate operations (note that the thermal fluctuation errors discussed above associated with T_r would also apply to the effective temperature of an additional drive field). The simplest way to accomplish this would be to drive the resonator *instead* of the qubits, and use the qubit/resonator coupling to accomplish the modulation of $\hat{\eta}$ for the gate. In table I we list the quantity N_γ , the resonator photon number (at ω_d) required to produce the full qubit bias swing necessary for each set of gate parameters. In nearly all of the cases considered, these values are comparable to or larger than the $\sim 10^3 - 10^4$ photons typically necessary to saturate the resonator loss in current experiments.

One disadvantage of this scheme is that by driving the resonator, all qubits connected to it would necessarily become entangled. In architectures where this would be a problem, an alternative method would be to drive the resonator with a separate, *resonant* drive (i.e., at $\bar{\omega}_r$) to saturate its loss, while driving only the desired qubits at ω_d ; to avoid spurious entanglement from the resonant drive in conjunction with a nonzero $\delta\omega_r^-$, one would need to invert the sign of this resonant drive in the middle of the gate, resulting in a classical “echo” similar to the method discussed above and shown in fig. 2(c).

The final issue we need to address is the presence of

higher modes in the resonator [12], which will also be displaced by interaction with the qubits, according to their effective capacitance (inductance for the magnetic case of fig. 1(b)) and geometrical coupling factors. The resulting (state-dependent) excursions do not in general decouple from the qubit at the same time as the fundamental mode, leaving a spurious entanglement between the qubits and the higher modes. Working in our favor, as in the atomic case [14–17] is the fact that the excursion of higher modes is suppressed by detuning, by at least a factor δ_d for transmission-line resonators with equidistant harmonics, and potentially significantly more for the lumped case. Using eq. 17 for the error due to a state dependent excursion $\delta\alpha_k^-$ of mode k with frequency $\omega_{r,k} \equiv f_k\omega_r$, and taking $\delta\alpha_k^-$ to be $\sim \eta_{ac,k}^-$ the effective Lamb-Dicke parameter for that mode [c.f., eq. 11]:

$$\epsilon_{hm} \sim \frac{(\eta_{0,k}^-)^2(1+2\bar{n})}{2(1-f_k^{-2})^2} \quad (23)$$

Using this result, we list in table I the minimum separation Δ_{hm} from the fundamental to the next higher mode, assuming that $\eta_{0,k}^- = \eta_0^-$, which would give rise to an error ϵ_{hm} *one tenth* of the total error from all other

sources. In all cases $\Delta_{hm} < \omega_r$, indicating these errors are unlikely to be significant in practical cases.

IV. CONCLUSION

The method we have presented here has some favorable advantages compared to the analogous techniques demonstrated with trapped atomic ions. For example, in our case, the resonator modes are nearly (though not completely) independent of the qubits, so that adding more qubits does not generate additional nearby collective modes which must be avoided as in the case of trapped ions. Also, in the ion case the equivalent controlled-phase interaction requires the ions to be in magnetic field sensitive states, which produces inevitable dephasing [14]; in our proposal, although the states used must also be field-sensitive, the sign of their sensitivity is oscillating at a high frequency so that to leading order dephasing is nearly absent (except in qubits with no degeneracy point). Although alternative methods for ions have been demonstrated that use states without field sensitivity [15, 16], they have additional complications which limit the gate speed, fidelity, and number of ions that can be entangled [16]. Finally, although the schemes used for ions are nominally insensitive to the state of the resonator, they still require a small Lamb-Dicke parameter, meaning that the ions must be localized to a much smaller region than the laser wavelength to avoid sampling a spatially dependent force [16]. This can be particularly challenging in the context of the ubiquitous heating observed in ion traps, which causes η to increase in time, in the absence of active laser cooling [49]. In our case, although η is also a small parameter (in the expansion $E_{g,e}(p)$), this expansion does not break down as in the atomic case; in fact, most of the error sources we have discussed actually *decrease* with larger η . In the expansion of eq. 2, we included terms up to second order in the resonator displacement δQ_r , and for the parameters in table I the errors associated with the second order term [c.f., eqs. 19,20] are already small enough for low error rates. Under these conditions, third and higher-order terms have a negligible effect [50].

Our method also has some potentially useful advantages over the current cQED paradigm for qubit-resonator coupling [6, 7]. Since no photons are exchanged between qubits and resonator, there is no Purcell effect [12], and the qubits' excited-state lifetimes are decoupled both from the qubit-resonator detuning, and from the resonator Q . It also avoids the relatively small on/off coupling ratios encountered in cQED architectures where the coupling is controlled only by detuning qubits from cavities [11, 51]. Furthermore, unlike in circuit QED where spurious population of excited photon states of the resonator directly produces gate errors, our scheme can tolerate even substantial thermal occupation of excited resonator states (up to $\bar{n} = 0.4$ was considered in table I), as well as coherent driving of the resonator, with

low impact on gate fidelity in the cases we have considered. This removes the need for an extremely low effective resonator temperature and/or a high resonator frequency (i.e., $T_r \ll \hbar\omega_r/k_B$), and also in some cases the need to operate the resonator in the single-photon limit where high Q is more difficult to achieve.

In closing, we note that the geometric phase of eq. 13 can be generalized to N qubits [c.f., eq. 8], giving an effective interaction $\propto (\sum_i \hat{\sigma}_i^z)^2$. This type of many-qubit interaction may be of interest, for example, in cluster-state generation [52], or syndrome extraction in quantum error-correction schemes where multiqubit operators are required, such as surface codes [53].

Note added - An error-suppression method closely related to that shown in fig. 2(c) was recently demonstrated for trapped atomic ions in [D. Hayes, S.M. Clark, S. Deb-nath, D. Hucul, I.V. Inlek, K.W. Lee, Q. Quraishi, and C. Monroe. Phys. Rev. Lett. **109**, 020503 (2012)].

We acknowledge helpful discussions with and/or comments from Daniel Greenbaum, Arthur Kerman, and Adrian Lupascu. This work is sponsored by the Assistant Secretary of Defense for Research & Engineering under Air Force Contract #FA8721-05-C-0002. Opinions, interpretations, conclusions and recommendations are those of the author and are not necessarily endorsed by the United States Government.

Appendix: Details on error estimates

1. Superconducting qubits

For the flux qubits [fig. 1(f)], we take $E_J/h = 200$ GHz, $E_C/h = 5.7$ GHz, and $\alpha(\Phi_{b0}) = 0.74$. This gives $\omega_{qb}(\Phi_{b0})/2\pi = 4.73$ GHz and $L_q^- = 15.9$ nH, $L_q^+ = 0$ [56]. We assume a drive amplitude of $\delta\Phi_{AC} = 0.1\Phi_0$, corresponding to $\alpha(0.1\Phi_0) = 0.70$ and $\omega_{qb}(0.1\Phi_0) = 7.8$ GHz. For the transmons [fig. 1(e)], we take $\omega_{qb}(\Phi_{b0} = 0)/2\pi = 15$ GHz, which gives $L_q^- = L_q^+/2 = -2(\Phi_0/\pi)^2/\hbar\omega_p = -87.4$ nH. Here we assume a drive excursion $\delta\Phi_{AC} = 0.2\Phi_0$, corresponding to $\omega_{qb}(0.2\Phi_0) = 13.5$ GHz. For both flux and transmon qubits we take $L_c = 25$ pH [57]. Also for both of these cases we must consider the effect of junction asymmetry in the DC SQUID (defined by the area asymmetry parameter: $A_J \equiv 2(A_1 - A_2)/(A_1 + A_2)$), which produces a spurious coupling between external flux and the SQUID plasma mode. For the limit $L_c \ll L_J$ satisfied here, we find the matrix element for the drive to couple to the first excited vibrational state of the plasma mode: $M_A \approx (\delta\Phi_{AC}/\Phi_0)A_J\sqrt{\pi/4\hbar\omega_p}$. We then have a maximal probability in this excited state of $\sim (\pi/4)(\delta\Phi_{AC}/\Phi_0)^2 A_J^2 (\omega_p/(\omega_p - \omega_d))^2$. Thus, for $A_J < 0.05$ and $\delta\Phi_{AC}/\Phi_0 < 0.2$, this error is at the 10^{-4} level or below. This calculation also gives a residual, direct Jaynes-Cummings type coupling between DC SQUID plasma mode and the resonator: $g \approx \omega_p \beta_r A_J \sqrt{Z_r/8R_Q}$, which can be neglected in the cases considered here.

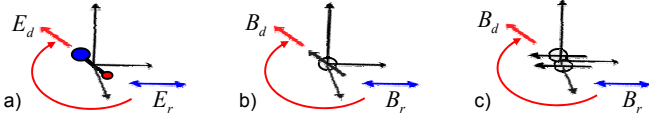


FIG. 3: Orientation of vector qubits driven by rotating fields. (a) trapped molecular ion qubits, and (b) electron spin qubits driven by a rotating field E_d or B_d , respectively, whose rotation plane contains the resonator mode field direction; in both cases the dipole orientation follows the drive field. In (c), the NV center spin triplet is driven by a rotating magnetic field B_d whose rotation plane contains the resonator mode field (B_r) direction; the orientation (quantization axis) of the NV center is determined by the crystal, and is also contained in the drive field's rotation plane.

2. Singlet-triplet coupled quantum dots

Figure 1(g): The singlet-triplet coupled quantum dots (and molecular ions below) are biased with a voltage, rather than a charge, so that: $C_b, C_c \gg C_q$ (the opposite limit from the superconducting qubit cases). In this limit, the voltages across C_b, C_c can be neglected, and $V_q \approx V_b$. The quasicharge is then: $Q_q \approx dE^-/dV_q$ evaluated at V_b . The displacement of the resonator in eq. 3 is then $C_q V_b$ and instead of eqs. 2 and 8, we have: $\eta_0^- \equiv (dE^-/dV_q)/(2\sqrt{\hbar Y_r})$, $C_q^- \equiv d^2 E^-/dV_q^2$, and $\delta\omega_r^-/\omega_r \approx -C_q^-/(2C_r)$. For the quantum dots we use the parameters of ref. 28, with a tunneling amplitude of $t_c = 23\mu\text{eV}$. We take an exchange energy J for each qubit which oscillates from $\sim 1\mu\text{eV}$ to $\sim 2.5\mu\text{eV}$, corresponding to electrode voltages from -0.7mV to -0.4mV , dE^-/dV_e from $0.002e$ to $0.01e$, and $C_q^- = 2C_q^+ \sim 1$ to 10 aF .

3. Trapped molecular ions

Figure 1(h): The trapped polar molecular ions of ref. 2 have a vector dipole moment, associated here primarily with the $J = 1$ excited molecular rotational manifold with sublevels $m_J = -1, 0, 1$ which are degenerate at zero electric field. An electric field shifts the $J = 1, m_J = \pm 1$ levels down, so that a qubit can be realized with the $J = 0, m_J = 0$ and $J = 1, m_J = 0$ states. We therefore cannot simply oscillate the electric field through zero, since the $m_J = 0$ state will undergo Majorana-like transitions to the $m_J = \pm 1$ states near zero field (equivalently, the induced dipole's orientation will not “follow” the applied field). Instead, we can use a *rotating* electric field E_d with angular frequency ω_d , whose plane of rotation contains the resonator mode field axis as shown in fig. 3(a). In this case, as long as the rotation is not too fast, the molecular dipole will follow it, resulting in an oscillating projection of the dipole along the resonator mode field. The effect of the rotation can be expressed via Larmor's theorem as an effective magnetic field along the rotation axis: $B_{\text{rot}} = \hbar\omega_d/\gamma_{J=1}$ where $\gamma_{J=1}$ is the gyromagnetic ratio of the $J = 1$ manifold. As long as the rotation is turned on and

off slowly, and we restrict ourselves to $\hbar\omega_d \lesssim E_{m_J=0} - E_{m_J=\pm 1}$, the states will transform adiabatically.

With this in mind, we take $E_d = 2.5\text{ kV/cm}$, corresponding to a differential stark shift between the $J = 0, m_J = 0$ and $J = 1, m_J = 0$ rotational states from their zero-field splitting of 9 GHz to $\sim 13\text{ GHz}$, and a splitting between $J = 1, m_J = 0$ and $J = 1, m_J = \pm 1$ of $\sim 3\text{ GHz}$; we take a distance $l = 1\mu\text{m}$ between the qubits and drive electrodes, so that $V_b \sim E_d l$.

Finally, although the rotation at constant field magnitude E_d does not couple the $J = 0, m_J = 0$ to the $J = 1$ manifold, there is a residual direct Jaynes-Cummings type coupling between the resonator and the $J = 0 \leftrightarrow J = 1$ transition, given by: $\hbar g \approx (d_{01}/l)\sqrt{\hbar Y_r}/C_r = 0.4\text{ MHz}$ ($d_{01} \approx 2.5 \times 10^{-29}\text{C}\cdot\text{m}$ is the transition dipole between $J = 0$ and $J = 1$); this produces a negligible effect at the large qubit-resonator detunings $\gtrsim 10\text{ GHz}$ considered here.

4. Donor electron spins in Si

Figure 1(i): Similar to the case of quantum dots and molecular ions which are biased with a voltage or electric field rather than a charge, an electron spin is biased with a magnetic field rather than a flux. In this case, we have: $\eta_0^- \equiv (dE^-/dI_q)/(2\sqrt{\hbar Z_r})$, $L_q^- \equiv d^2 E^-/dI_q^2$, and $\delta\omega_r^-/\omega_r \approx -L_q^-/(2L_r)$. We take a circular loop of diameter $d = 50\text{nm}$ connected to the resonator, with the spin at its center, so that the field at the spin is given by: $B_d = \mu_0 I_q/d$. As in the case of molecular ions, a rotating field (turned on and off slowly) must be used to avoid Majorana transitions between spin orientations [fig. 3(b)], whose rotation frequency in this case should be less than the Larmor frequency $\omega_L = \gamma_e B_d/\hbar$. For our drive at 1 GHz , we then select a field amplitude of $B_d = 1000\text{G}$, corresponding to $\omega_L/2\pi = 2.8\text{ GHz}$. At this field, the hyperfine splitting of $\approx 117\text{ MHz}$ [58] produces a negligible $L_q^- \approx 10^{-22}\text{H}$. Our chosen parameters $Q = 10^7$, $d = 50\text{ nm}$, and $B_d = 1000\text{G}$, while arguably not completely implausible, are admittedly extreme. The very weak interaction with a single spin dictates that such parameters are required for favorable gate parameters. One way to relax these requirements to some extent would be to implement a multiturn coil (it would need to be at the $\sim 100\text{nm}$ scale) to increase the coupling, or to use an ensemble of spins as a qubit.

5. Nitrogen vacancy centers in diamond

Figure 1(j): This case is similar to the electron spin just discussed, except that the system is a spin triplet with $S = 1$, and the $m_S = 0$ state is shifted relative to the $m_S = \pm 1$ states due to crystal-field and magnetic-dipole interactions by 2.88 GHz [59]. The axis of this internal field is fixed by the crystal, so that the alignment of the states cannot follow the external drive field direction for

weak fields. However, if we align the resonator mode field along the NV center's crystal axis, and use a drive field rotation plane that also contains this axis [fig. 3(c)], we can still realize the desired effect (we take as above $B_d = 1000\text{G}$). When the drive field B_d is along the crystal axis, the resonator field produces a linear Zeeman shift of the $m_S = \pm 1$ states; when the drive field is perpendicular to the axis, it mixes all three sublevels, producing a large enough avoided crossing that the $m_S = \pm 1$ states can be

nearly adiabatically transformed into each other by the drive, and we can use them as our two qubit states (Note that in experiments, the $S = 0, m_s = 0$ state is typically used as $|g\rangle$). As above, this can be fully accounted for using an effective field associated with the rotation. As long as the drive frequency is not too large, and the drive is as above turned on and off slowly, nonadiabatic transitions can be neglected at the error levels of interest here.

-
- [1] I. Buluta, S. Ashhab, and F. Nori, Rep. Prog. Phys., **74**, 104401 (2011), and references therein.
 - [2] D.I. Schuster, L.S. Bishop, I.L. Chuang, D. DeMille, and R.J. Schoelkopf, Phys. Rev. A **83**, 012311 (2011).
 - [3] A. André, D. DeMille, J. M. Doyle, M. D. Lukin, S. E. Maxwell, P. Rabl, R. J. Schoelkopf, and P. Zoller, Nature Phys **2**, 636 (2006).
 - [4] S.D. Hogan, J.A. Agner, F. Merkt, T. Thiele, S. Filipp, and A. Wallraff, Phys. Rev. Lett. **108**, 063004 (2012); C. Guerlin, E. Brion, T. Esslinger, and K. Mølmer, Phys. Rev. A **82**, 053832 (2010); D. Petrosyan, G. Bensky, G. Kurizki, I. Mazets, J. Majer, and J. Schmiedmayer, Phys. Rev. A **79**, 040304(R) (2009); A.S. Sørensen, C.H. van der Wal, L.I. Childress, and M.D. Lukin, Phys. Rev. Lett. **92**, 063601 (2004).
 - [5] J.M. Raimond, M. Brune, and S. Haroche, Rev. Mod. Phys. **73**, 565 (2001).
 - [6] A. Blais, R.-S. Huang, A. Wallraff, S.M. Girvin, and R.J. Schoelkopf, Phys. Rev. A **69**, 062320 (2004); D.I. Schuster, A. Wallraff, A. Blais, L. Frunzio, R.-S. Huang, J. Majer, S.M. Girvin, and R.J. Schoelkopf, Phys. Rev. Lett. **94**, 123602 (2005).
 - [7] A. Wallraff, D.I. Schuster, A. Blais, L. Frunzio, R.-S. Huang, J. Majer, S. Kumar, S.M. Girvin and R.J. Schoelkopf, Nature **431**, 162 (2004); J.Q. You and F. Nori, Nature **474**, 589 (2011) and references therein.
 - [8] D.I. Schuster, *et al.*, Phys. Rev. Lett. **105**, 140501 (2010).
 - [9] P. Bushev, A.K. Feofanov, H. Rotzinger, I. Protopopov, J.H. Cole, C.M. Wilson, G. Fischer, A. Lukashenko, and A.V. Ustinov, Phys. Rev. B **84**, 060501(R) (2011).
 - [10] R. Miller, T.E. Northup, K.M. Birnbaum, A. Boca, A.D. Boozer, and H.J. Kimble, J. Phys. B: At. Mol. Opt. Phys. **38**, S551 (2005).
 - [11] An exception is in [S.J. Srinivasan, A.J. Hoffman, J.M. Gambetta, and A.A. Houck, Phys. Rev. Lett. **106**, 083601 (2011)].
 - [12] A.A. Houck, *et al.*, Phys. Rev. Lett. **101**, 080502 (2008).
 - [13] A.P. Sears, A. Petrenko, G. Catelani, L. Sun, H. Paik, G. Kirchmair, L. Frunzio, L.I. Glazman, S.M. Girvin, and R.J. Schoelkopf, Phys. Rev. B **86**, 180504(R) (2012); A. Palacios-Laloy, F. Mallet, F. Nguyen, F. Ong, P. Bertet, D. Vion and D. Esteve, Phys. Scr. **T137**, 014015 (2009); A. Córcoles, J.M. Chow, J.M. Gambetta, C. Rigetti, J.R. Rozen, G.A. Keefe, M.B. Rothwell, M.B. Ketchen, and M. Steffen, Appl. Phys. Lett. **99**, 181906 (2011).
 - [14] D. Leibfried, *et al.*, Nature **422**, 412 (2003).
 - [15] P.C. Haljan, K.-A. Brickman, L. Deslauriers, P.J. Lee, and C. Monroe, Phys. Rev. Lett. **94**, 153602 (2005).
 - [16] K. Mølmer and A. Sørensen, Phys. Rev. Lett **82**, 1835 (1999); A. Sørensen and K. Mølmer, Phys. Rev. A **62**, 022311 (2000).
 - [17] G. J. Milburn, S. Schneider, and D.F.V. James, Fortschr. Phys. **48**, 801 (2000).
 - [18] Related methods specific to Josephson-junction-based “flux” qubits were described in: [Y.X. Liu, L.F. Wei, J.R. Johansson, J.S. Tsai, and F. Nori, Phys. Rev. B **76**, 144518 (2007); Y.-D. Wang, A. Kemp, and K. Semba, Phys. Rev. B **79**, 024502 (2009)].
 - [19] The original proposal for trapped-ion entangling gates [J.I. Cirac and P. Zoller, Phys. Rev. Lett. **74**, 4091 (1995)] relied on direct exchange of internal excitations of the ions with their collective vibrational modes, and required these modes to have almost zero temperature to achieve high gate fidelity. In this, it was similar to some early cQED realizations of coupled superconducting qubits which relied on real exchange of photons between qubits and resonator [e.g., M.A. Sillanpää, J.I. Park, and R.W. Simmonds, Nature **449**, 438 (2007)].
 - [20] Qubit-state-dependent resonator displacements can also be realized in the dispersive limit of cQED [21] by driving the resonator and using the qubit-induced dispersive shift to achieve a state-dependent result. In refs. 21 this idea was used for manipulation or measurement of a resonator state by a single qubit. This method is distinct from our proposal, in that it involves virtual exchange of photons and can be viewed as a nonlinear response of the system to a resonator drive. By contrast, in the present work the force on the resonator is explicitly qubit-state-dependent, the system remains linear, and only the qubits are driven.
 - [21] Z. Leghtas, G. Kirchmair, B. Vlastakis, M. Devoret, R. Schoelkopf, and M. Mirrahimi, arXiv:1205.2401; M. Pechal, S. Berger, A.A. Abdumalikov, Jr., J.M. Fink, J.A. Mlynek, L. Steffen, A. Wallraff, and S. Filipp, Phys. Rev. Lett. **108**, 170401 (2012).
 - [22] K.K. Likharev, IEEE Trans. Mag. **23**, 1142 (1987); A.M. Kadin, J. Appl. Phys **68**, 5741 (1990); J.E. Mooij and Yu.V. Nazarov, Nature Physics **2**, 169 (2006).
 - [23] K.K. Likharev and A.B. Zorin, J. Low. Temp. Phys. **59**, 347 (1985); W. Guichard and F.W.J. Hekking, Phys. Rev. B **81**, 064508 (2010); A.J. Kerman, arXiv:1201.1859.
 - [24] Note that in (b) we have used inductive dividers (rather than mutual inductances) to retain exact duality with the capacitive circuit of (a); however, mutual inductances can also be used with straightforward modifications to the results presented here.
 - [25] M.H. Devoret, in “Quantum Fluctuations”, Les Houches summer school 1995, eds. S. Reynaud, E. Giacobino, and

- J. Zinn-Justin.
- [26] F. G. Paauw, A. Fedorov, C. J. P. M. Harmans, and J. E. Mooij, *Phys. Rev. Lett.* **102**, 090501 (2009).
 - [27] T.P. Orlando, J.E. Mooij, L. Tian, C.H. van der Wal, L.S. Levitov, S. Lloyd, and J.J. Mazo, *Phys. Rev. B* **60**, 15398 (1999).
 - [28] J.R. Petta, A.C. Johnson, J.M. Taylor, E.A. Laird, A. Yacoby, M.D. Lukin, C.M. Marcus, M.P. Hanson, and A.C. Gossard, *Science* **309**, 2180 (2005); E.A. Laird, J.R. Petta, A.C. Johnson, C.M. Marcus, A. Yacoby, M.P. Hanson, and A.C. Gossard, *Phys. Rev. Lett.* **97**, 056801 (2006).
 - [29] B.M. Maune, *et al.*, *Nature* **481**, 344 (2012).
 - [30] M.D. Shulman, O.E. Dial, S.P. Harvey, H. Bluhm, V. Umansky, and A. Yacoby, *Science* **336**, 202 (2012).
 - [31] M. Steger, K. Saeedi, M.L.W. Thewalt, J.J.L. Morton, H. Riemann, N.V. Abrosimov, P. Becker, and H.-J. Pohl, *Science* **336**, 1280 (2012).
 - [32] G. Balasubramanian, *et al.*, *Nat. Materials* **8**, 383 (2009).
 - [33] Note that C_b does not contribute to C'_r because the qubit voltage V_q is effectively fixed.
 - [34] C.E. Weiman, D.E. Pritchard, and D.J. Wineland, *Rev. Mod. Phys.* **71**, S253 (1999).
 - [35] J.D. Miller, R.A. Cline, and D.J. Heinzen, *Phys. Rev. A* **47**, 4567(R), (1993).
 - [36] There is also an analogy with our system for case (i), which allows resolved-sideband cooling of the resonator. Sidebands of this kind have in fact been observed in a superconducting circuit: [D. Gunnarsson, J. Tuorila, A. Paila, J. Sarkar, E. Thuneberg, Y. Makhlin, and P. Hakonen, *Phys. Rev. Lett.* **101**, 256806 (2008)].
 - [37] See, e.g., D.F. Walls and G.J. Milburn, *Quantum Optics*, Springer 1994.
 - [38] This type of interaction (which commutes with the qubit Hamiltonians) has been considered for a single qubit in [G. Vacanti, R. Fazio, M.S. Kim, G.M. Palma, M. Paternostro, and V. Vedral, *Phys. Rev. A* **85**, 022129 (2012)] as a way to measure geometric phases of a resonator; it has also been used as a means to couple two qubits to each other via a third qubit in [A.J. Kerman and W.D. Oliver, *Phys. Rev. Lett.* **101**, 070501 (2008)].
 - [39] We note that eq. 7 fully describes the classical, linear dynamics of of interest here at *any* resonator amplitude (as long as the resonator itself is linear). This is in contrast to the cQED case, where the Jaynes-Cummings nonlinearity becomes important as the amplitude is increased [see, e.g., L.S. Bishop, E. Ginossar, and S.M. Girvin, *Phys. Rev. Lett.* **105**, (2010)]. Classical behavior is also recovered in the high-temperature limit $T_r \gg \hbar\omega_r/k_B$, discussed in [S.N. Shevchenko, A.N. Omelyanchouk, and E. Il'ichev, *Low. Temp. Phys.* **38**, 283 (2012)].
 - [40] It is also possible to simply turn a force on for a fixed time, with no oscillatory component [Sasura and Steane, *Phys. Rev. A* **67**, 062318]; this method provides no discrimination between the desired resonator mode and higher modes, and requires an η larger by a factor δ_d^{-1} .
 - [41] G. Ithier, *et al.*, *Phys. Rev. B* **72**, 134519 (2005).
 - [42] A. Megrant, *et al.*, *Appl. Phys. Lett.* **100**, 113510 (2012).
 - [43] A. Gilchrist, N.K. Langford, and M.A. Nielsen, *Phys. Rev. A* **71**, 062310 (2005).
 - [44] By defining the error in this way, we are neglecting any long-term quantum coherence of the oscillator, and assuming that its coupling to the environment will produce decay to a statistical mixture of coherent states, the so-called “pointer states” of the system [J.R. Anglin and W.H. Zurek, *Phys. Rev. D*, **53**, 7327 (1996)].
 - [45] Gh.-S. Paraoanu and H. Scutaru, *Phys. Rev. A* **58**, 869 (1998).
 - [46] The classical evolution of the coherent state α_0 does not cause decoherence in the manner that thermal photon number fluctuations do, since it is deterministic and taken into account by the state-dependent frequency shift $\delta\hat{\omega}_r$ and corresponding displacement δv_q^- .
 - [47] Note that with negligible transverse coupling, noise at ω_{qb} does not induce the usual enhanced spontaneous decay (Purcell effect) encountered in circuit QED [12].
 - [48] M.J. Biercuk, H. Uys, A.P. VanDevender, N. Shiga, W.M. Itano, and J.J. Bollinger, *Nature* **458**, 996 (2009); J. Bylander, S. Gustavsson, F. Yan, F. Yoshihara, K. Harrabi, G. Fitch, D.G. Cory, Y. Nakamura, J.-S. Tsai, and W.D. Oliver, *Nature Physics* **7**, 565 (2011).
 - [49] D.A. Hite, *et al.*, *Phys. Rev. Lett.* **109**, 103001 (2012).
 - [50] A correction which can in principle be important would be a strong *quartic* term in the qubit energy, which results in a modulation of ω_r at *twice* ω_d , *parametrically* exciting the oscillator. We have simulated this, and it is negligible for the parameters considered here.
 - [51] F. Helmer, M. Mariani, A.G. Fowler, J. von Delft, E. Solano, and F. Marquardt, *Europhys. Lett.* **85**, 50007 (2009); A. Galiutdinov, A.N. Korotkov, and J.M. Martinis, *Phys. Rev. A* **85**, 042321 (2012); D. DiVincenzo, *Phys. Scr.* **T137**, 014020 (2009).
 - [52] E. Kuznetsova, T. Bragdon, R. Coté, and S.F. Yelin, *Phys. Rev. A* **85**, 012328 (2012).
 - [53] R. Raussendorf and J. Harrington, *Phys. Rev. Lett.* **98**, 190504 (2007).
 - [54] For example, A.J. Kerman, E.A. Dauler, W.E. Keicher, J.K.W. Yang, K.K. Berggren, G. Gol'tsman, and B. Voronov, *Appl. Phys. Lett.* **88**, 111116 (2006); R. Barends, N. Vercruyssen, A. Endo, P.J. de Visser, T. Zijlstra, T.M. Klapwijk, P. Diener, S.J.C. Yates, and J.J.A. Baselmans, *Appl. Phys. Lett.* **97**, 023508 (2010); A. Kamlapure, M. Mondal, M. Chand, A. Mishra, J. Jesudasan, V. Bagwe, L. Benfatto, V. Tripathi, and P. Raychaudhuri, *Appl. Phys. Lett.* **96**, 072509 (2010); B. Baek, A.E. Lita, V. Verma, and S.W. Nam, *Appl. Phys. Lett.* **98**, 251105 (2011); M. Sandberg, M.R. Vissers, J.S. Kline, M. Weides, J. Gao, D.S. Wisbey, and D.P. Pappas, *Appl. Phys. Lett.* **100**, 262605 (2012).
 - [55] A.J. Kerman, *Phys. Rev. Lett.* **104**, 027002 (2010).
 - [56] For the flux qubit calculations, we use the numerical methods described in ref. 55
 - [57] With DC SQUID junction capacitances of $C_J \sim 3\text{fF}$ this gives a plasma frequency for the circulating mode of $1/2\pi\sqrt{L_c C_J/2} = 0.8\text{ THz}$, so that the driving considered here will negligibly excite it.
 - [58] M.L.W. Thewalt, *et al.*, *J. Appl. Phys.* **101**, 081724 (2007).
 - [59] J. Wrachtrup, S.Ya. Kilin, and A.P. Nizovtsev, *Opt. and Spectrosc.* **91**, 429 (2001).